EPJ Web of Conferences **303**, 04001 (2024) https://doi.org/10.1051/epjconf/202430304001
MENU 2023

Combined analysis of K^-p reactions and $\pi\Sigma$ photoproduction data

Aleš Cieplý[1,*] and *Peter C.* Bruns[1]

[1]Nuclear Physics Institute of the Czech Academy of Sciences, 250 68 Řež, Czechia

Abstract. We discuss results of a simultaneous fit to the K^-p reactions and $\pi\Sigma$ photoproduction data employing an approach that combines tree level photoproduction amplitudes with $\pi\Sigma - \bar{K}N$ coupled channel model describing the meson-baryon rescattering in the final state. The achieved reproduction of the photoproduction mass distributions represents a significant improvement when compared with the parameter free predictions made earlier but remains inferior to more comprehensive models that employ much larger sets of adjustable parameters.

1 Motivation

The modern treatment of meson-baryon (MB) interactions at low energies is based on Chiral Perturbation Theory (ChPT) which is used in combination with multi-channel techniques to calculate the MB scattering amplitudes. In this approach, the $\pi\Sigma - \bar{K}N$ coupled channel dynamics generates two poles in the isoscalar sector that can be assigned to the $\Lambda(1405)$ resonance. The *higher mass* pole that is closer to the real axis is often interpreted as a K^-p quasi-bound state, while the other more distant pole was assigned recently to a newly introduced $\Lambda(1380)$ state. Unfortunately, the experimental data (K^-p reaction cross sections, threshold branching ratios, and kaonic hydrogen characteristics) used so far to fit the $\pi\Sigma-\bar{K}N$ coupled channel models are not restrictive enough, so the theoretical predictions for the $\bar{K}N$ amplitudes exhibit large variations at subthreshold energies as well as in the isovector sector [1]. A similar uncertainty also applies to the position of the $\Lambda(1380)$ pole [2].

It was suggested in [3] that the mentioned model dependence could be reduced by fitting the free parameters of the $\pi\Sigma - \bar{K}N$ coupled channel model not only to the experimental data available in the K^-p sector, but complementing them with the existing data on $\pi\Sigma$ photoproduction that cover the energies below the K^-p threshold dominated by the $\Lambda(1405)$ resonance. In fact, the CLAS data for the $\gamma p \to K^+\pi\Sigma$ cross sections [4] were already used to separate several χ^2 local minima found in the K^-p fits [5] assuming a general ad-hoc form for the photoproduction part of the process. Several other photoproduction models were also tested and their predictions compared with the CLAS data [6–8], all of them relying on MB rescattering amplitudes generated by $\pi\Sigma - \bar{K}N$ models fitted exclusively to the K^-p data.

The photoproduction reaction $\gamma p \to K^+MB$ is illustrated in Fig. 1. There, the MB scattering amplitudes $\mathcal{T}$ can be implemented to describe the final-state interaction of the produced MB pair. The $\mathcal{M}$-bubble represents the first part of the process, the tree level photoproduction amplitudes. In the early works [5, 6] this part was modeled utilizing quite simple

*e-mail: cieply@ujf.cas.cz

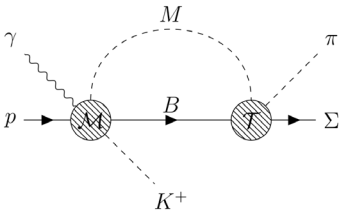

Figure 1. Illustration of the final-state interaction (FSI) of the meson-baryon pair. $\mathcal{M}$ represents the amplitude for the $\gamma p \to K^+ MB$ without FSI, and $\mathcal{T}$ is the meson-baryon scattering amplitude.

energy dependent phenomenological form while the later approaches [7, 8] constructed the photoproduction amplitudes in a more sophisticated manner, though still required an introduction of energy-dependent phenomenological terms. Finally, the approach adopted in [3, 9] constructs the photoproduction kernel $\mathcal{M}$ from tree level graphs derived from baryon ChPT adhering strictly to constraints arising from unitarity and gauge invariance. While in [3] the authors discussed the impact of the MB final state interactions on the $\pi\Sigma$ mass spectra and revealed large variations of the results for different $\pi\Sigma - \bar{K}N$ models, the work [9] represents a first genuine attempt to use the CLAS photoproduction data [4] in fits of the MB model parameters. In the present contribution we briefly recap the latter work and discuss its results.

2 Results

The formalism adopted in [3] does not contain any free parameter but was found lacking in reproducing the experimental $\pi\Sigma$ line-shapes and completely inadequate to emulate the energy dependence yielding too large cross sections at higher energies. Therefore, additional form-factors were introduced in [9] and applied to the photoproduction kernel $\mathcal{M}$, impacting also on the regularization of the intermediate MB loop function connecting the photo-kernel with the rescattering amplitude $\mathcal{T}$. The regularization scales of these form factors complement the parameters of the Prague model [10] used to generate the MB scattering amplitudes in the FSI. In addition one more form factor was introduced in [9] for the outgoing spectator kaon. All form factors were taken in the Yamaguchi form, matching the one used for the separable MB amplitudes in the Prague $\pi\Sigma - \bar{K}N$ model, see the details in [9, 10].

The fitted experimental data include the available data from two sectors:

- $K^- p$ reactions: low energy total cross sections to different MB states ($MB = \pi^0\Lambda$, $\pi^0\Sigma^0$, $\pi^-\Sigma^+$, $\pi^+\Sigma^-$, $K^- p$, $\bar{K}^0 n$, $\eta\Lambda$, $\eta\Sigma^0$), three threshold branching ratios (γ, R_c and R_n) and the kaonic hydrogen characteristics ($1s$ level energy shift ΔE_N and absorption width Γ due to strong interaction), see [9, 10] for the references to the data origins
- $\pi\Sigma$ photoproduction: $\pi\Sigma$ mass spectra measured by the CLAS collaboration at the $\sqrt{s} = 2.1$ GeV energy [4]

In total 252 data points for 13 observables were fitted, each observable represented by a set of data points contributing with the same weight to the total χ^2 per degree of freedom. The free parameters adjusted to the data comprised of 6 regularization scales defining the separable MB FSI amplitudes, 6 low energy constants representing couplings of the NLO MB chiral Lagrangian, and 4 newly introduced scales (for the $\pi\Lambda$, $\pi\Sigma$, $\bar{K}N$ channels, and for the outgoing K^+ meson) in the form factors applied to the photoproduction $\mathcal{M}$ amplitudes. Several other parameters of the model were kept fixed, see [9] for more details.

In Table 1 and Fig. 2 we show the achieved results for four selected χ^2 minima representing models P0, P1, P2 and P3. In the first P0 model the meson-baryon amplitudes used in the FSI were kept fixed, generated by the Prague model specified in [10], and four scales introduced to augment the $\mathcal{M}$ amplitudes were varied. Thus, the pertinent $\chi^2/\mathrm{dof} = 5.40$ is higher and not directly comparable with the values reached in the other fits. Having the LECs and FSI scales fixed for the $\mathcal{T}$ amplitudes also means that the P0 model generates exactly the same results in the sector of K^-p reactions as the original Prague model of Ref. [10]. The other three models P1, P2 and P3 were obtained while varying all 16 parameters. In Table 1 we also present the χ^2/dof calculated separately for the K^-p reactions and the $\pi\Sigma$ photoproduction data. There, the numbers of observables and parameters utilized in each sector are different from the overall fit, $N_{obs} = 10$ and $N_{par} = 12$ for the K^-p, and $N_{obs} = 3$ and $N_{par} = 16$ for the $\pi\Sigma$ sectors. It is clearly seen that the description of the K^-p reactions data is reasonable while the unsatisfactory high χ^2/dof ($\pi\Sigma$) values spoil the overall fit as well.

Table 1. The reproduction of the K^-p threshold data (branching ratios γ, R_c and R_n, $1s$ level energy shift ΔE_N and absorption width Γ) and the positions of the dynamically generated poles on the *second Riemann sheet*. The results are shown for 4 selected model fits providing the local minima with the χ^2/dof given in the second line. The following two lines refer to the χ^2 criteria applied selectively on the K^-p reactions and the $\pi\Sigma$ photoproduction data, respectively.

model	P0	P1	P2	P3
χ^2/dof	5.40	3.34	4.41	4.72
χ^2/dof (K^-p)	1.52	1.93	2.06	2.74
χ^2/dof ($\pi\Sigma$)	19.2	9.14	13.9	12.9
$\gamma = 2.36 \pm 0.04$	2.37	2.37	2.37	2.36
$R_c = 0.664 \pm 0.011$	0.656	0.663	0.647	0.646
$R_n = 0.189 \pm 0.015$	0.208	0.194	0.204	0.213
$\Delta E_N = 283 \pm 42$ eV	307	305	309	354
$\Gamma = 541 \pm 111$ eV	589	616	611	557
$\Lambda(1380)$: z_1 [MeV]	(1353, 43)	—	(1347, 71)	(1345, 58)
$\Lambda(1405)$: z_2 [MeV]	(1428, 24)	(1421, 43)	(1425, 46)	(1425, 45)
$\Lambda(1670)$: z_3 [MeV]	(1677, 14)	—	(1725, 57)	(1665, 7)

The results shown in Table 1 demonstrate that all considered models reproduce quite well the experimental data at the K^-p threshold. Similarly, it was shown in [3] that the K^-p total cross sections are also well reproduced by the models. However, the P1 model representing the global χ^2 minimum was found unphysical for two reasons. First of all, as one can immediately see in Table 1, the model generates only one isoscalar pole, missing on the poles assigned to $\Lambda(1380)$ and $\Lambda(1670)$. This is in stark contrast with the other models as well as with a general belief that the $\pi\Sigma - \bar{K}N$ coupled channel models derived from chiral Lagrangian generate two isoscalar poles below the K^-p threshold. A closer examination of the P1 solution also revealed that it generates an isovector pole quite close to the real axis and in a vicinity of the $\pi\Sigma$ threshold, leading to a narrow spike in the MB amplitudes involving the isovector component. As no such isovector state is known in the discussed energy region, the P1 solution is clearly unphysical. However, the fact that the P1 model reproduces the K^-p data about equally well (if not even better) as the other models, can be interpreted in a way that the K^-p data set does not restrict sufficiently the theoretical models used in the analysis.

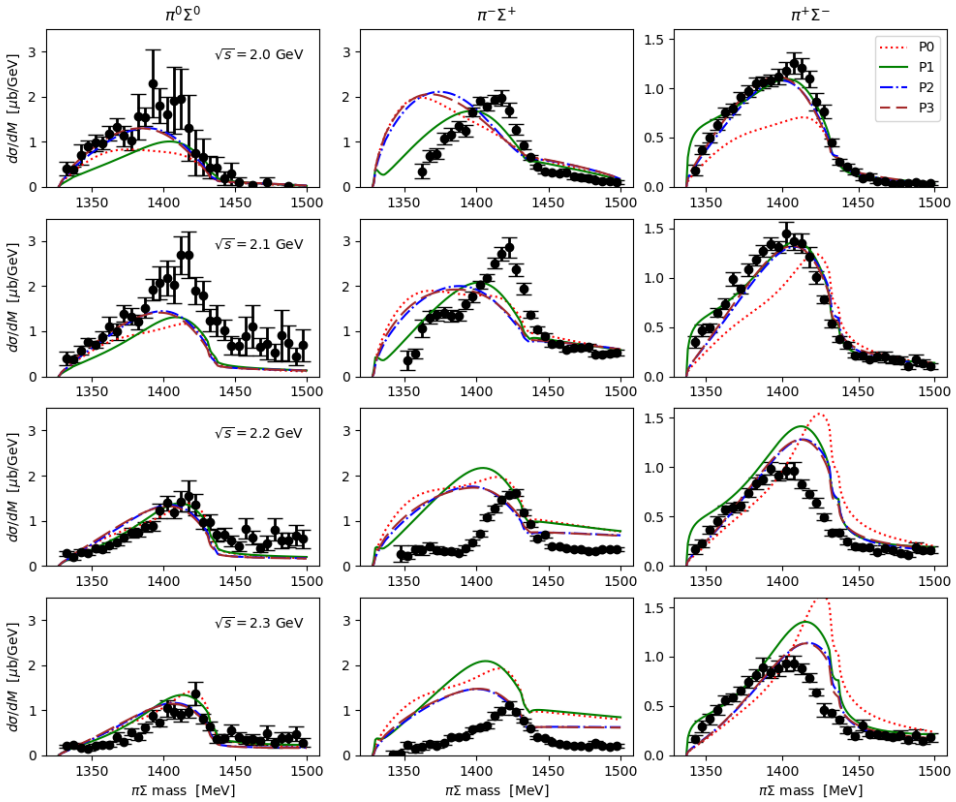

Figure 2. A comparison of the generated $\pi\Sigma$ mass distribution with the CLAS data. The subfigures are arranged in rows and columns according to the pertinent c.m. energy $\sqrt{s}$ and channel, respectively.

In this respect, we clearly need more new experimental data for the $\bar{K}N$ reactions at as low kaon momenta as possible.

Concerning the z-values of the Λ^* poles presented in Table 1 it is worth noting the clustering of the P1, P2 and P3 $\Lambda(1405)$ pole positions at about the same complex energy but with about twice as large imaginary part when compared with the P0 model prediction (and those by other groups) that was based solely on fits of the K^-p reactions data. The predictions of the $\Lambda(1380)$ position also appear to be more constrained than in previous analyses aiming exclusively at reproducing the K^-p data.

The reproduction of the CLAS photoproduction data is shown in Fig. 2 for the c.m. energies $\sqrt{s} \leq 2.3$ GeV (only the data at $\sqrt{s} = 2.1$ GeV were fitted). Considering that our treatment of the photo-kernel, the $\mathcal{M}$ amplitude in Fig. 1, is relatively simple and only four parameters were fitted besides those already used in the $\pi\Sigma - \bar{K}N$ coupled channels model, the description of the $\pi^0\Sigma^0$ and $\pi^+\Sigma^-$ mass distributions is quite reasonable. The energy dependence (the magnitude of the generated spectra) is also under control, mostly due to introducing the form-factor related to the kaon emission. Unfortunately, the model fails to reproduce the $\pi^-\Sigma^+$ mass distributions. As a result, the overall description of the $\pi\Sigma$ mass spectra is not satisfactory, which is reflected by relatively high values of the χ^2 criteria shown in Table 1, especially those applied exclusively to the $\pi\Sigma$ sector. It is also puzzling that the $\pi^-\Sigma^+$ cross sections reported by the CLAS collaboration seem to start about 30 MeV above the channel

threshold while our theoretical models predict a steep rise right from the threshold energy. At the moment we have no proper explanation for this mismatch.

It should be noted that much better description of the CLAS data was obtained in previous works on the $\gamma p \to K^+\pi\Sigma$ photoproduction that introduced more graphs in the photo-kernel, including e.g. exchanges of vector mesons [7] or triangle diagrams [8]. However, the respective models were fitted with much larger sets of free parameters (many of them energy dependent) to achieve a good reproduction of the data. In contrast, our approach employs very limited number of parameters (none of them energy dependent), so it is understandable that the presented models do not describe the CLAS data so well.

3 Summary

We have reported on a first-time attempt to fit simultaneously the low energy K^-p reactions data together with the $\pi\Sigma$ mass spectra observed in the photoproduction on protons. Although we have not managed to bring the calculated $\pi\Sigma$ mass distributions into satisfactory agreement with the CLAS data, especially in the $\pi^-\Sigma^+$ channel, we believe the results demonstrate the viability of the chosen approach. The local χ^2 minima found in our work agree on the position of the *higher mass* $\Lambda(1405)$ pole at $z \approx (1425, -45)$ MeV and the mass of the $\Lambda(1380)$ seems to be restricted to the interval $\mathrm{Re}\, z \approx 1350\pm10$ MeV. Though, it is difficult to draw any definite conclusions regarding the pole positions before accomplishing better data reproduction.

The description of the $\pi\Sigma$ mass distributions may be improved by considering additional contributions in the ab-initio construction of the photoproduction kernel, the $\mathcal{M}$ amplitudes. In particular, the graphs involving vector mesons and decuplet baryons in the intermediate states should play a non-negligible role. A work in this direction is in progress.

Acknowledgement

A.C. acknowledges support received from the European Union's Horizon 2020 research and innovation program under grant agreement No 824093.

References

[1] A. Cieplý, M. Mai, U.G. Meißner, J. Smejkal, Nucl. Phys. A **954**, 17 (2016), 1603.02531
[2] M. Mai, Eur. Phys. J. ST **230**, 1593 (2021), 2010.00056
[3] P.C. Bruns, A. Cieplý, M. Mai, Phys. Rev. D **106**, 074017 (2022)
[4] K. Moriya et al. (CLAS), Phys. Rev. C **87**, 035206 (2013), 1301.5000
[5] M. Mai, U.G. Meißner, Eur. Phys. J. A **51**, 30 (2015), 1411.7884
[6] L. Roca, E. Oset, Phys. Rev. C **88**, 055206 (2013), 1307.5752
[7] S.X. Nakamura, D. Jido, PTEP **2014**, 023D01 (2014), 1310.5768
[8] E. Wang, J.J. Xie, W.H. Liang, F.K. Guo, E. Oset, Phys. Rev. C **95**, 015205 (2017), 1610.07117
[9] A. Cieplý, P.C. Bruns, Nucl. Phys. A **1043**, 122819 (2024), 2305.06205
[10] P.C. Bruns, A. Cieplý, Nucl. Phys. A **1019**, 122378 (2022), 2109.03109